Aerosol and Air Quality Research

ORIGINAL RESEARCH
https://doi.org/10.4209/aaqr.210294

Planetary Boundary Layer and its Relationship with $PM_{2.5}$ Concentrations in Almaty, Kazakhstan

Madina Tursumbayeva[1,2], Aiymgul Kerimray[2*], Ferhat Karaca[3,4], Didin Agustian Permadi[5]

[1] Department of Meteorology and Hydrology, Al-Farabi Kazakh National University, Almaty, Kazakhstan
[2] Center of Physical Chemical Methods of Research and Analysis, Al-Farabi Kazakh National University, Almaty, Kazakhstan
[3] School of Engineering and Digital Science, Department of Civil and Environmental Engineering, Nazarbayev University, Nur-Sultan, Kazakhstan
[4] The Environment and Resource Efficiency Cluster, Nazarbayev University, Nur-Sultan, Kazakhstan
[5] Institut Teknologi Nasional, Bandung, Indonesia

ABSTRACT

Air pollution is a severe problem in Almaty (Kazakhstan), especially during the cold half of the year (October-March). Almaty is one of the most polluted cities in Kazakhstan and Central Asia, with average winter $PM_{2.5}$ (particulate matter with aerodynamic diameter ≤ 2.5 µm) concentration of 94.0 µg m^{-3}. High pollution in the wintertime in Almaty could be caused by emissions from coal combustion for power and heat generation (at power plants and small-scale heating), which could also be worsened by poor dispersion of air pollutants due to certain atmospheric conditions. Based on one-year radiosonde data, the characteristics of the planetary boundary layer height (PBLH) and its effect on ground-level $PM_{2.5}$ concentrations in Almaty were analyzed in this study using the bulk Richardson number (Ri) and potential temperature increase (PT) methods. During an annual cycle, the concentrations of $PM_{2.5}$ were highest in the winter months when the daily concentrations were above 100 µg m^{-3} for 38 days during this period. The results show a clear negative relationship between the daily average $PM_{2.5}$ concentrations and PBLH at 12.00 UTC. For instance, high $PM_{2.5}$ concentrations in winter months (94.0 µg m^{-3}) corresponded to a lower PBLH (393 m), and low $PM_{2.5}$ concentrations in summer months (9.9 µg m^{-3}) corresponded to a higher PBLH (1970 m). During the cold half of the year, the top 20% of $PM_{2.5}$ concentrations were associated with a lower PBLH and calm wind conditions (lower average wind speeds within the PBL and a lower ventilation coefficient). The results show that PBLH variations during the year have a significant effect on $PM_{2.5}$ concentrations; however, further analysis is needed with a more substantial amount of observational data to understand this interaction further and to investigate the role of synoptic processes that lead to a shallow PBLH.

Keywords: Air quality, Pollution, Planetary boundary layer height, $PM_{2.5}$, Kazakhstan

OPEN ACCESS

Received: December 5, 2021
Revised: May 4, 2022
Accepted: June 1, 2022

[*] Corresponding Author:
aiymgul.kerimray@cfhma.kz

Publisher:
Taiwan Association for Aerosol Research
ISSN: 1680-8584 print
ISSN: 2071-1409 online

1 INTRODUCTION

Almaty, the former capital and largest city in Kazakhstan, has been experiencing a period of rapid urbanization since the independence of the country in 1991. This growth has been a reason for several environmental problems where the most serious one is atmospheric pollution during the cold half of the year. Today, with a population of more than 2 million people (Committee of Statistics of the Ministry of the National Economy of the Republic of Kazakhstan, 2021), Almaty is considered as one of the most polluted cities in Kazakhstan (Russell *et al.*, 2018), with concentrations of particulate matter with aerodynamic diameter ≤ 2.5 µm ($PM_{2.5}$) in some days higher than 250 μg m^{-3} (Kerimray *et al.*, 2020a). Nationally, air pollution in Kazakhstan leads to 10,064 premature deaths, and the economic damage due to air pollution in Kazakhstan (including indoor air pollution) was estimated at US $29.2 billion per year, or 9.3% of GDP (as of 2010) (WHO Regional Office for Europe, 2015). Aerosols have significant impact on precipitation, cloud, and climate radiative forcing (Koren *et al.*, 2014; Permadi *et al.*, 2018a; Li *et al.*, 2019a; Guo *et al.*, 2019). Thus, reducing air pollutant emissions will decrease air pollution, improve public health, and benefit the economy. The major emission sources of $PM_{2.5}$ in Almaty include coal-fired power plants, domestic heating stoves using coal, and vehicle exhaust (Kerimray *et al.*, 2020a). Annually, two coal power plants in Almaty (CHP-2 and CHP-3) use approximately 3.4 million tons of coal, and advanced emission control systems are not employed (electrostatic precipitators and flue gas desulfurization are not used). The volumes of coal consumption at CHPs depend on the ambient temperature because combined heat and power plants provide heat to district heating systems. Almaty's climatic conditions, where the long-term average temperatures in January and July are –4.7 and 23.9°C, respectively (Pogoda I Climate, 2021), show that there is a considerable need for heating during the cold half of the year. Because of this, the average daily coal consumption is twice as high in January than in June at Almaty CHP-2. In addition, Almaty is located in the foothills of the northern part of the Tian Shan mountain system at 600 m above sea level. The city's location restricts both the vertical and horizontal dispersion of air pollutants emitted from the ground level. These meteorological and topographic conditions, combined with local emission build-up that is similar to Ulaanbaatar (Wang *et al.*, 2017), contribute to the high concentration of $PM_{2.5}$.

Numerous studies have focused on determining meteorological factors influencing the spatial and temporal distributions of particulate matter (especially $PM_{2.5}$) in recent years worldwide (Wangc *et al.*, 2014; Wang *et al.*, 2017; Li *et al.*, 2019b). The growing interest in $PM_{2.5}$ is driven by the damaging impact of pollutants on human health, which has been reported in many epidemiological studies (Kampa and Castanas, 2008). $PM_{2.5}$ was found to be the fifth-ranking global mortality factor that caused 7.6% of total deaths worldwide in 2015 (Cohen *et al.*, 2017). Haze pollution leads to an increased risk of morbidity and hospital admissions; respiratory, cardiovascular, and cerebrovascular diseases; lung cancer; and premature death (Gao *et al.*, 2017; Yin *et al.*, 2020). To the authors' knowledge, research on the spatial and temporal variations in catmospheric pollutants in Kazakhstan cities (Kerimray *et al.*, 2020b) and their effect on human health (Vinnikov *et al.*, 2020; Kenessary *et al.*, 2019) is limited, and an assessment of $PM_{2.5}$ relationships with meteorological parameters (e.g., planetary boundary layer height) in Almaty has yet to be performed (Ormanova *et al.*, 2020).

The planetary boundary layer height (PBLH) is one of the most critical meteorological factors limiting the vertical mixing of air pollutants, including $PM_{2.5}$, near the surface. Since the PBLH cannot be directly measured, several other methods have been introduced to obtain it, where the most common method is using radiosondes. They can measure vertical profiles of meteorological parameters on a sounding balloon and are usually launched twice daily (00 and 12 UTC) at most stations around the world (Guo *et al.*, 2021). After Holzworth's pioneering research on early radiosonde data over the US in 1964, research on PBLH assessment has constantly been progressing further. In addition to the parcel method (Holzworth, 1964), several other algorithms, such as the bulk Richardson number (Seidel *et al.*, 2012), temperature inversions (Hu *et al.*, 2014; Nielsen-Gammon *et al.*, 2008), and other methods, have been developed. New remote sensing techniques (lidars, wind profilers, ceilometers, and radiometers) have also been introduced for continuous PBLH measurements (Seibert *et al.*, 2000). The climatology of the PBL height over Europe and the continental United States was compiled by Seidel *et al.* (2012), over China by Guo *et al.* (2016), and over the Korean Peninsula by Allabakash and Lim (2020), and the global PBLH diurnal cycle was assessed by Gu *et al.* (2020) and Guo *et al.* (2021). A few pieces of research in Central Asia have also been reported from mountainous areas of Ulaanbaatar (Wang *et al.*, 2017) and Nur-Sultan, the capital city of Kazakhstan (Ormanova *et al.*, 2020). The results suggest the important contribution of the PBLH to the accumulation of $PM_{2.5}$ during certain seasons. Several modeling studies have indicated that the PBLH is one of the most sensitive meteorological parameters for simulating PM concentration (Permadi *et al.*, 2018a, 2018b). To date, no studies have been reported on the influence of the PBLH on particulate matter concentrations in Almaty, Kazakhstan.

The particulate matter pollution problem in Almaty shows a worsening trend; therefore, it is important to provide science-based evidence on the current status, as well as deriving a better understanding of the major contributing factors. This study explores the relationship between the PBLH and ground-level $PM_{2.5}$ concentrations in Almaty, Kazakhstan. In addition, the impact of wind speed is also discussed; therefore, the ventilation coefficient is characterized. Based on one-year radiosonde data, the PBLH was determined by applying the bulk Richardson number (Ri) and potential temperature increase (PT) methods. This analysis provides valuable information for understanding the seasonality of $PM_{2.5}$ pollution in relation to meteorological factors in Almaty; therefore, emission reduction measures can be formulated based on the key findings of this research.

2 METHODS

2.1 Data Collection

The data used in this study include surface meteorological data, $PM_{2.5}$ mass concentration data, and sounding data from March 1st, 2020, to February 28th, 2021. ***The radiosonde data*** used in this study were collected from the Almaty aerological station (University of Wyoming, 2020). The Almaty aerological station (43.35°N and 77.00°E) started conducting temperature-wind soundings in 1952. The station is located 15 km from the city center at 660 m above sea level. The aerological station consists of a small-sized aerological locator MARL-A (functioning since January 2010), radiosondes (PAZA-22, Aspan-15), and a hydrogen-generating system. The radiosonde data include vertical profiles of pressure, height, temperature, dew point temperature, humidity, and wind speed and direction twice a day at 00:00 and 12:00 UTC (06:00 and 18:00 Almaty time, respectively (UTC +6)). In total, 719 sounding profiles were used in this study, of which 355 sounding profiles were at 00:00 UTC and 364 sounding profiles were at 12:00 UTC. ***$PM_{2.5}$ data*** were obtained from the United States Embassy station in Almaty (AirNow, 2021) that started collecting $PM_{2.5}$ data on February 4th, 2020, with a temporal resolution of 1 h. The Embassy uses BAM (beta attenuation monitor) 1020, which is the U.S. EPA equivalent method (Met One Instruments, 2021), to measure and record PM concentration levels in a continuous mode in Almaty. The sensor is installed at Kazakh National Medical University (43.25°N and 76.93°E), located in the city center. ***Surface meteorological data***, including surface air temperature, humidity, wind speed and direction, and precipitation, were obtained from www.rp5.kz for a station located close to the aerological station in Almaty (43.35°N and 77.03°E). The website rp5.kz archives meteorological information from the international exchange data server at the National Oceanic and Atmospheric Administration, USA, since 2004 (Weather Schedule, 2021). The locations of the stations (aerological, meteorological, and $PM_{2.5}$) within Almaty districts are shown in Fig. 1. Descriptive statistics with the pollutant concentrations and meteorological data for the considered period are presented in Table S1.

2.2 Methods to Determine PBLH

This study used two PBLH detection methods: bulk Richardson number (Ri) and potential temperature increase (PT) methods. Both methods have been widely used in other studies for PBLH detection (Seidel *et al.*, 2012; Guo *et al.*, 2016; Miao *et al.*, 2018; Gu *et al.*, 2020). The Ri method is suitable for stable and convective conditions, which is defined as follows (Eq. (1)):

$$Ri(z) = \frac{\left(\frac{g}{\theta_{vs}}\right)(\theta_{vz} - \theta_{vs})(z - z_s)}{(u_z - u_s)^2 + (v_z - v_s)^2 + bu_*^2} \quad (1)$$

where g is gravity acceleration, θ_v is virtual potential temperature, *z* is height, *u* and *v* are wind components, *b* is a constant and u_* is surface friction velocity. The subscripts *s* and *z* denote the surface and height, respectively. Since u_* is not known from the radiosonde data, and its effect is much smaller than the bulk shear term in the denominator (Seidel *et al.*, 2012), *b* was set to 0, and the surface friction term was ignored. Then, PBLH was determined as the lowest level where

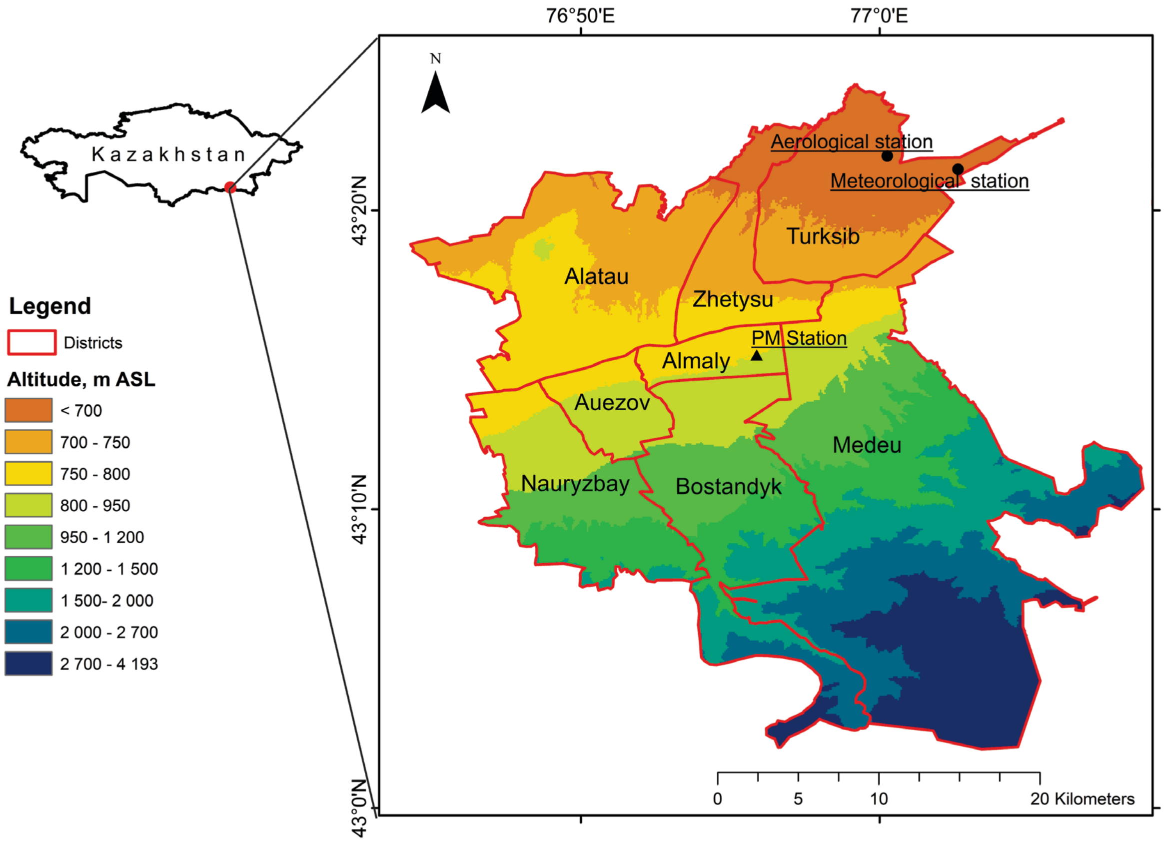

Fig. 1. Districts of Almaty with the elevation and location of PM and aerological and meteorological stations.

the *Ri*(*z*) value exceeded 0.25. This method has been used in several papers (Seidel *et al.*, 2012; Guo *et al.*, 2016; Miao *et al.*, 2018). All PBLHs in this study are presented in meters above ground level (m AGL).

PBLH was also estimated using the PT method (Nielsen-Gammon *et al.*, 2008; Su *et al.*, 2020; Miao *et al.*, 2018). Assuming that the potential temperature at the PBL top is higher than at the surface, the PBLH was determined as the level where the potential temperature first exceeds the surface potential temperature by more than 2 K (Fig. S1).

To learn the relationship between PBLH and $PM_{2.5}$ concentrations, after data normalization (using log-transformation), Pearson's linear correlation (R) coefficient was applied, and p values were calculated.

There were several terms used in this paper to describe time periods for (1) seasons: spring (March, April, and May), summer (June, July, and August), autumn (September, October, and November), and winter (December, January, and February) and (2) two halves of the year: cold half of the year (from October to March) and warm half of the year (from April to September).

3 RESULTS AND DISCUSSION

3.1 Meteorological Parameters

The location of Almaty in an area with a severe continental climate dictates the large differences between summer and winter temperature values. During the study period, the average monthly temperature values were lowest in December (–7.8°C) and January (–4.7°C) and highest in July (23.9°C) and August (23.5°C). The lowest average monthly wind speeds were observed from October to February, with the minimum in December (1.7 m s^{-1}). In addition, this period (from October to February) was characterized by the highest number of no-wind conditions, which may complicate the dispersion of pollutants during this period. In contrast, the relative humidity increased during the winter months (e.g., the maximum was in January [88%]), and the lowest values were from June to September (e.g., the minimum was in June [42%]). Precipitation during this period had seasonal fluctuations, with two peaks in April (237 mm) and February (130 mm). Thus, the winter months, December and January, when the $PM_{2.5}$ pollution is the heaviest, were characterized by the lowest temperature and wind speed values, and highest humidity values. Meteorological conditions for Almaty are summarized from March 1st, 2020, to February 28th, 2021 in Fig. 2.

The wind direction varied greatly from winter to summer (Fig. 3) during the study period. In winter, there was no prevailing wind direction, and the average wind speed was 1.9 m s^{-1}, while in summer and autumn, winds were mostly in a southern direction with average wind speeds of 2.6 m s^{-1} (summer) and 1.9 m s^{-1} (autumn). In spring, winds were in southern and western directions with average speeds of 2.6 m s^{-1}.

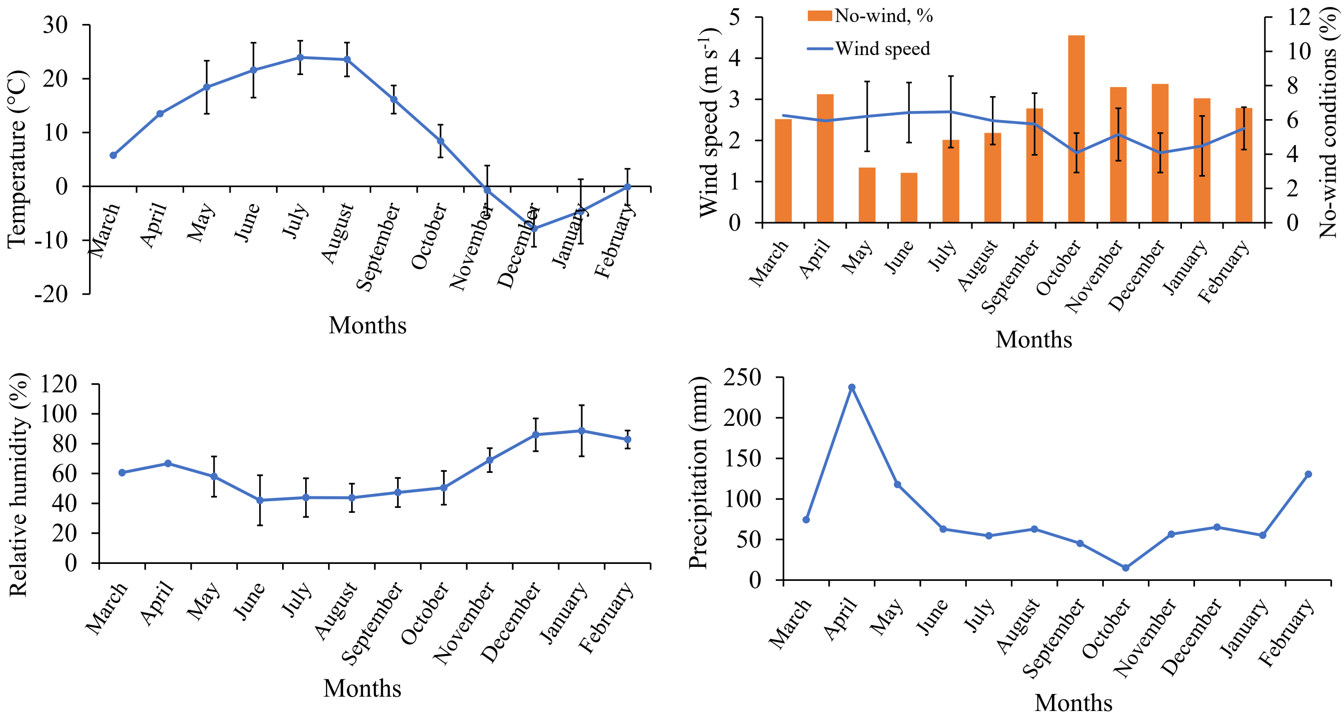

Fig. 2. Monthly average values of temperature, relative humidity, wind speed, and precipitation during 2020–2021.

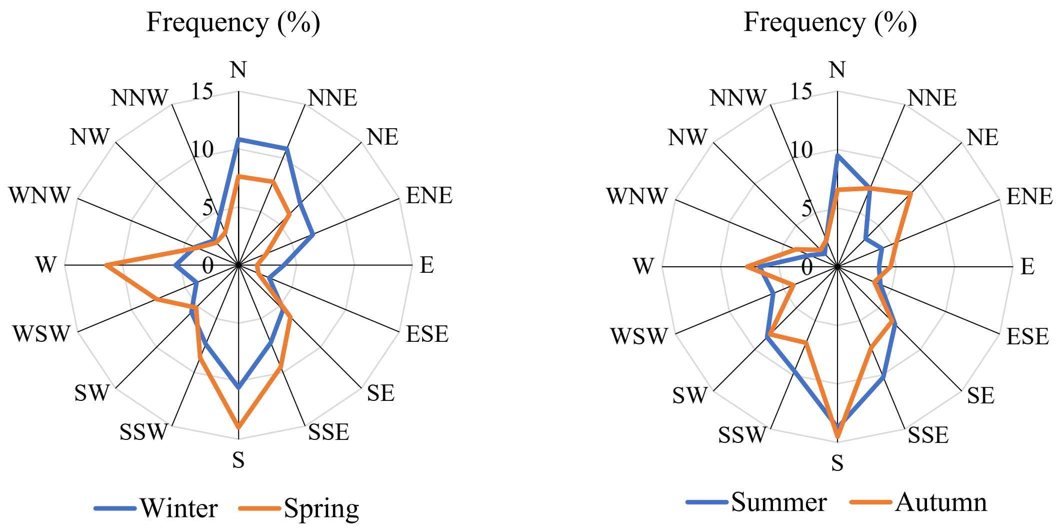

Fig. 3. Direction of wind for spring, summer, autumn and winter for the 2020–2021 period.

3.2 Variations of $PM_{2.5}$ Concentrations

The annual mean concentration of $PM_{2.5}$ for the selected period was 39.2 µg m^{-3}. There is no established national standard for annual $PM_{2.5}$ concentrations in Kazakhstan (only for daily and maximum one-time concentrations). However, the annual mean concentration is almost eight times higher than the annual standard established by WHO guidelines (5.0 µg m^{-3}) (WHO, 2021). The value of the annual concentration in Almaty (39.2 µg m^{-3}) was close to the annual concentration of $PM_{2.5}$ in Beijing in 2020 (38.8 µg m^{-3}) (Statista, 2021). In this work, the annual concentrations of $PM_{2.5}$ (39.2 µg m^{-3}) were lower than those in a study by Kerimray *et al.* (2020a) (53 µg m^{-3}). The reason for this could be that the $PM_{2.5}$ sensor used in this study was located in the higher part of the city (Almaly district), while in the study by Kerimray *et al.* (2020a), $PM_{2.5}$ data from several sensors in different parts of the city included sensors located in lower parts that were characterized by higher concentrations of $PM_{2.5}$.

Daily average concentrations did not meet the 24-hour concentration standards established by the WHO on most days from October to March. In addition, most days from the second half of October to the first half of March did not meet the national daily $PM_{2.5}$ standards of 35 µg m^{-3} (Adilet, 2021). Thus, during this period, citizens experienced exposure to high $PM_{2.5}$ concentrations that may induce a series of different adverse effects on public health (Feng *et al.*, 2016). Daily average concentrations of $PM_{2.5}$ are presented in Fig. 4.

The concentrations of $PM_{2.5}$ in Almaty showed significant variations during the year. During the cold half of the year (from October to March), the percentile analysis showed a long-tailed distribution: 92.8% of the days were characterized by average daily $PM_{2.5}$ concentrations higher than 15 µg m^{-3}, 65.3% were higher than 35 µg m^{-3}, 46.4% were higher than 50 µg m^{-3}, 23.2% were higher than 100 µg m^{-3}, and 8.3% were higher than 150 µg m^{-3}. In December and January, the average monthly concentrations were about 110 µg m^{-3}. In total, 24% of the days in those two months were characterized by daily average $PM_{2.5}$ concentrations of more than 150 µg m^{-3} with a maximum of 237 µg m^{-3} on December 24th, 2020. High $PM_{2.5}$ concentrations in Almaty could be related to increased coal combustion for heat generation and disadvantageous meteorological conditions during this period. On the other hand, lower $PM_{2.5}$ concentrations were observed from April to September. During this period, the daily average concentration exceeded the WHO daily standards in 19.3% of the days.

For the diurnal cycle, the $PM_{2.5}$ concentrations were the highest in the late evening and midnight throughout the year (Fig. 5). The lowest concentrations were found from 6 a.m. to 12 p.m. (Almaty time) from October to February and from 3 a.m. to 6 a.m. (Almaty time) from March to September (Table S2). Interestingly, during noon, a second peak was observed from April to September. It was not statistically reliable (1) to study the diurnal variation in the PBLH since sounding observations were performed only twice a day (at 00 and 12 UTC), which also did not represent the peak times; consequently, (2) there was uncertainty in the relationship between the PBLH and $PM_{2.5}$ concentrations during the day. More sounding observations are needed to understand this interaction further, especially during the cold half of the year when PM pollution is the heaviest.

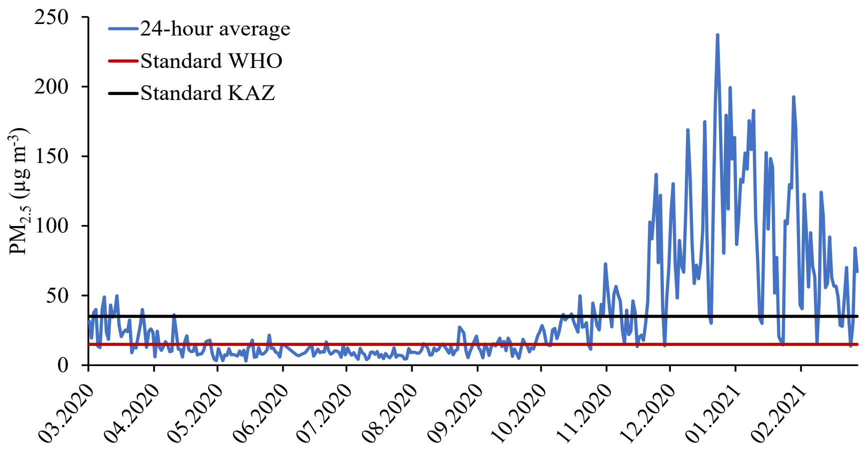

Fig. 4. 24-hour average $PM_{2.5}$ concentrations during March 2020–February 2021.

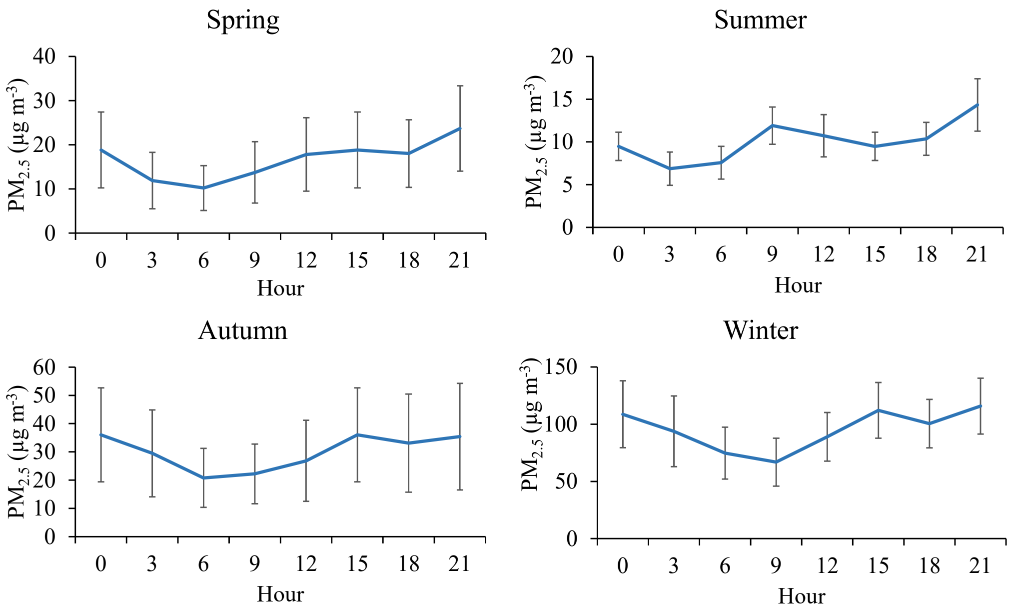

Fig. 5. Average $PM_{2.5}$ concentrations at synoptic hours for spring, summer, autumn and winter in 2020–2021.

3.3 Impact of the PBLH on $PM_{2.5}$ Concentrations

Based on sounding data, the average daily PBLH at 00:00 and 12:00 UTC (or 06:00 and 18:00 Almaty time) for the study period was calculated using both the Ri and PT methods. Although the results of the two methods were significantly correlated (P = 0.91 for 00:00 UTC and P = 0.71 for 12:00 UTC), the correlation between $PM_{2.5}$ and PBLH derived from the PT method was higher. The correlation coefficients derived from the two methods during cold (October–March) and warm (April–September) halves of the year are shown in Table 1. All correlation coefficients were negative. $PM_{2.5}$ concentrations had stronger anti-correlations with daily PBLH at 18:00 than at 06:00 (Almaty time). Since the PBLH at 00:00 UTC (06:00 Almaty time) did not significantly affect the concentrations, the PBLH derived with the PT method at 12:00 UTC (18:00 Almaty time) was used in further analyses.

Fig. 6 illustrates the average heights of the PBL at 00:00 and 12:00 UTC (06:00 and 18:00 Almaty time) and $PM_{2.5}$ concentrations from March 1st, 2020, to February 28th, 2021. The average PBLHs at 12:00 UTC had clear seasonal patterns, with the maximum height during summer (average 1969 m) followed by spring (average 1748 m) and autumn (average 1137 m). The minimal PBLHs were observed during the winter months (average 392 m). The average PBLHs at 00:00 UTC did not show a clear seasonal pattern as those at 12:00 UTC, and they varied from 134 to 265 m. $PM_{2.5}$ concentrations reached their maximum during winter (average 94.0 μg m^{-3}), followed by autumn (average 30.5 μg m^{-3}). Lower concentrations were observed during summer (average 9.9 μg m^{-3}) and spring (average 16.9 μg m^{-3}). The comparison between the PBLH at 12:00 UTC and $PM_{2.5}$ concentrations indicated obvious anti-correlation, suggesting that a higher PBLH corresponded to lower $PM_{2.5}$ concentrations.

The seasonal variations in the PBLH, average wind speed within the PBL, and ventilation coefficient

Table 1. Correlation between $PM_{2.5}$ and PBLHs derived from both the Ri and PT methods during cold (October–March) and warm (April–September) halves of the year. Numbers in bold show statistically significant correlations at a 95% confidence level.

Period	Method	00:00 UTC	12:00 UTC
October–March	Ri	–0.04	**–0.38**
	PT	–0.14	**–0.54**
April–September	Ri	0.07	–0.03
	PT	–0.01	–0.07

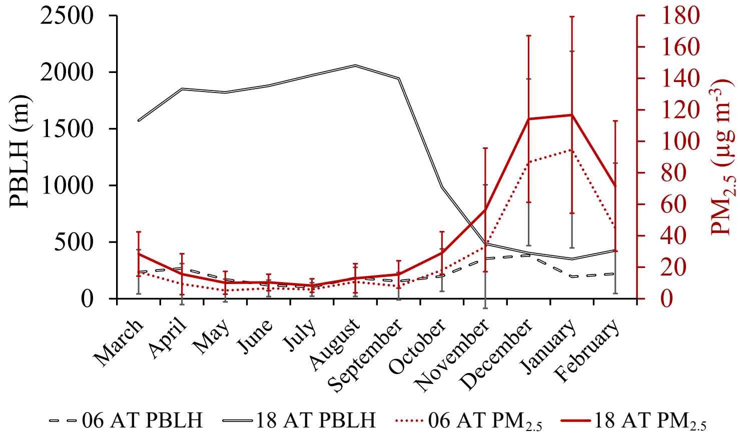

Fig. 6. Seasonal variations in PBLH and $PM_{2.5}$ concentrations in Almaty for the 2020–2021 period.

Table 2. Seasonal variation in PBLH, average wind speed within the PBL, and ventilation coefficient.

Seasons	Average PBLH (m AGL)	Average $PM_{2.5}$ (μg m^{-3})	Average wind speed (m s^{-1})	Ventilation coefficient (m^2 s^{-1})
Spring	1747.7	16.9	3.8	6892
Summer	1969.4	9.9	4.3	8952
Autumn	1137.4	30.5	3.7	5252
Winter	392.5	94.0	2.8	1274

Note: The ventilation coefficient was calculated by multiplying the PBLH by the wind speed within the PBL.

or air outflow are presented in Table 2. The ventilation coefficient was calculated as the product of the PBLH and average wind speed within the PBL. The results revealed that the average wind speed and ventilation coefficient were minimal in wintertime when the PBLH was lowest. Thus, the average wind speed and ventilation coefficient in winter were 2.8 m s^{-1} and 1274 m^2 s^{-1}, respectively.

In contrast, the highest values of wind speed (4.3 m s^{-1}) and ventilation coefficient (8951.9 m^2 s^{-1}) were observed during summer. The average wind speed and ventilation coefficient values in spring and autumn were in between but still considerably higher than those in winter. A lower ventilation coefficient is associated with weaker turbulence and stronger stability, which constrains the diffusion process of pollutants and contributes to higher concentrations of $PM_{2.5}$. The highest value of the ventilation coefficient during summer showed the best dispersion condition, which led to a normally lower concentration of $PM_{2.5}$. A higher $PM_{2.5}$ concentration during winter was somehow well correlated with a low ventilation coefficient value (1,274 m^2 s^{-1}), which represented a period of poor air mass dispersion.

3.4 PBL Structure in the Cold Half of the Year

To further understand the relationship between the PBLH and $PM_{2.5}$ concentrations, especially during the cold half of the year, PBLH characteristics were analyzed for the top and bottom 20% $PM_{2.5}$ daily concentrations. Initially, only the highest and lowest 20% of winter $PM_{2.5}$ concentrations were selected. However, the lowest 20% $PM_{2.5}$ concentrations ranging from 13 to 51 μg m^{-3} during the winter of 2020–2021 were caused mainly by heavy precipitation rather than changes in the PBLH (Fig. S2). When precipitation days were excluded, $PM_{2.5}$ concentrations for the bottom 20% started from approximately 50 μg m^{-3} (Figs. S2(b) and S2(c)). Since winter concentrations on no precipitation days were all above 50 μg m^{-3}, it was decided to extend the period from the winter to the cold half of the year (from October to March). Then, the top 20% of $PM_{2.5}$ concentrations ranged from 127 to 237 μg m^{-3}, while the bottom 20% ranged from 11 to 28 μg m^{-3} (Fig. 7). When the top 20% occurred, the PBLHs were lower than 500 m AGL with lower wind speeds and ventilation coefficients within the PBL. In some cases, low PBLH levels were accompanied by low concentrations and vice versa. This suggests that although PBLH plays a critical

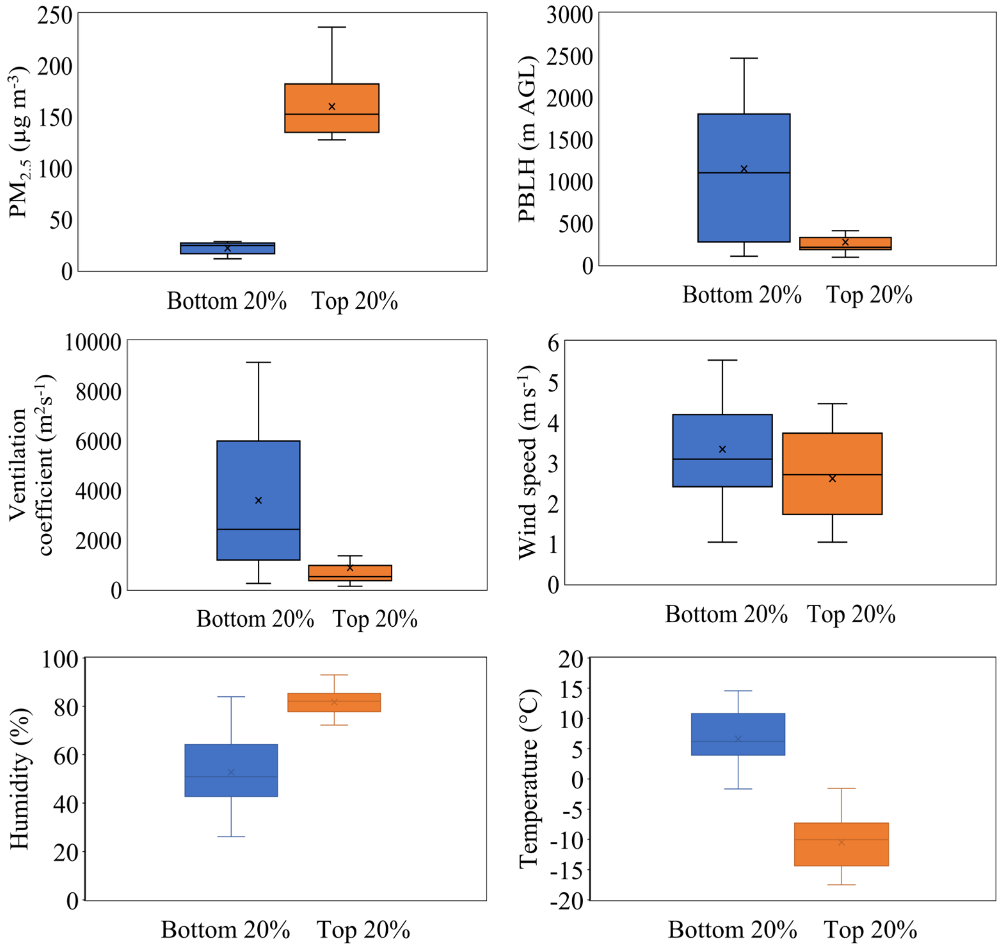

Fig. 7. The lowest (bottom 20%) and highest (top 20%) concentrations of $PM_{2.5}$ were associated with their different characteristics, such as PBLH, ventilation coefficient, wind speed within the PBL, and surface temperature and humidity.

role in the dispersion of air pollutants, $PM_{2.5}$ levels also depend on other factors (emission sources, meteorology, etc.). A shallow PBLH, lower wind speeds, and ventilation coefficient contributed to poorer conditions for the dispersion of air pollutants at ground level and resulted in days with the top 20% of $PM_{2.5}$ concentrations. In contrast, the bottom 20% corresponded to a higher PBLH, wind speed, and ventilation coefficient.

The relationship of the PBLH with temperature and humidity was also examined for the bottom and top 20% of $PM_{2.5}$ concentrations. The PBLHs at 12.00 UTC were positively correlated with surface temperature and inversely proportional to humidity. Thus, when the temperature was low, coal combustion for heating increased, and a shallow PBLH did not allow pollutants to be diluted, which resulted in pollutants accumulating in a very thin layer above the ground. The relative humidity during this period was approximately 70% to 95% in the top 20%, which was much higher than that in the bottom 20% (25% to 80%).

4 CONCLUSIONS

This paper used multiple datasets from a surface meteorological station, $PM_{2.5}$ monitoring station, and a sounding station to investigate the relationship between the PBLH and $PM_{2.5}$ concentrations in Almaty, one of the most populated and polluted cities in Kazakhstan.

There is severe air quality degradation in Almaty. The annual mean $PM_{2.5}$ concentration for March 2020–February 2021 was 39.2 μg m^{-3}, almost eight times higher than the annual limits for $PM_{2.5}$ established by the WHO.

During an annual cycle, the concentrations of $PM_{2.5}$ were highest in the winter months. On most days, 24-hour concentrations from October to March also did not meet the daily limits established by the WHO (92.8% of the days) and national limits of Kazakhstan (65.3% of the days). A total of 23.2% of the days during this period were characterized with concentrations higher than 100 $\mu g\ m^{-3}$. During the other months, the daily average concentration exceeded the WHO daily standards on 19.3% of the days. The average monthly concentrations were 110.7 $\mu g\ m^{-3}$ in December, 110.8 $\mu g\ m^{-3}$ in January, and 61.3 $\mu g\ m^{-3}$ in February. The decrease in $PM_{2.5}$ concentrations in February could have been associated with an increase in the height of the PBLH, intense precipitation, increasing ambient temperature and a reduction in coal use for heating. The lowest concentrations were observed in summer (9.9 $\mu g\ m^{-3}$). The average concentrations in spring and autumn were 16.9 and 30.5 $\mu g\ m^{-3}$, respectively.

In the wintertime, higher emissions of $PM_{2.5}$ from coal combustion at large-scale (power plants) and small-scale heating sources (heating stoves) contributed to air quality degradation. Meteorological and geographic conditions could also have contributed to winter peaks of $PM_{2.5}$ concentrations. The results show a clear negative relationship between the daily average $PM_{2.5}$ concentrations and PBLH at 12.00 UT. Thus, high $PM_{2.5}$ concentrations in winter months (94.0 $\mu g\ m^{-3}$) corresponded to a lower PBLH (392.5 m), and low $PM_{2.5}$ concentrations in summer months (9.9 $\mu g\ m^{-3}$) corresponded to a higher PBLH (1969.4 m).

During the day, $PM_{2.5}$ concentrations were the highest in the late evening and midnight throughout the year during the study period. The lowest concentrations were found from 6:00 a.m. to 12:00 p.m. (Almaty time) from October to February and from 3:00 a.m. to 6:00 a.m. (Almaty time) from March to September. Interestingly, during noon, a second peak was observed from April to September. It was not possible to study the diurnal variation in the PBLH and its effect on $PM_{2.5}$ concentrations since sounding observations were performed only twice a day. Thus, it would be beneficial to add sounding observations at 14:00 (Almaty time), especially during the cold half of the year when PM pollution is heaviest.

During the cold half of the year, the top 20% of $PM_{2.5}$ concentrations were associated with a lower PBLH and calm wind conditions (lower average wind speeds within the PBL and a lower ventilation coefficient).

The results of this study show the role of the PBLH in the formation of higher $PM_{2.5}$ concentrations. Further analysis is needed with a larger amount of observational data to understand this interaction further and to investigate the role of synoptic processes that lead to a shallow PBLH during cold periods.

ACKNOWLEDGMENTS

This work of Aiymgul Kerimray and Madina Tursumbayeva was funded by the Science Committee of the Ministry of Education and Science of the Republic of Kazakhstan (Grant No. AP09260359). The authors would like to thank the Ministry of Education and Science of the Republic of Kazakhstan for supporting Madina Tursumbayeva with a Ph.D. scholarship at Al-Farabi Kazakh National University.

SUPPLEMENTARY MATERIAL

Supplementary material for this article can be found in the online version at https://doi.org/10.4209/aaqr.210294

REFERENCES

Adilet (2021). On the approval of Hygienic standards for atmospheric air in urban and rural settlements. https://adilet.zan.kz/rus/docs/V1500011036

AirNow (2021). AirNow Department of State. https://www.airnow.gov/international/us-embassies-and-consulates/#Kazakhstan$Almaty

Allabakash, S., Lim, S. (2020). Climatology of planetary boundary layer height-controlling meteorological parameters over the Korean Peninsula. Remote Sens. 12, 2571. https://doi.org/10.3390/rs12162571

Cohen, A.J., Brauer, M., Burnett, R., Anderson, H.R., Frostad, J., Estep, K., Balakrishnan, K., Brunekreef, B., Dandona, L., Dandona, R., Feigin, V., Freedman, G., Hubbell, B., Jobling, A., Kan, H., Knibbs, L., Liu, Y., Martin, R., Morawska, L., Pope, C.A., *et al.* (2017). Estimates and 25-year trends of the global burden of disease attributablec to ambient air pollution: an analysis of data from the Global Burden of Diseases Study 2015. Lancet 389, 1907–1918. https://doi.org/10.1016/S0140-6736(17)30505-6

Committee of Statistics of the Ministry of the National Economy of the Republic of Kazakhstan (2021). https://stat.gov.kz/region/268020

Feng, S., Gao, D., Liao, F., Zhou, F., Wang, X. (2016). The health effects of ambient $PM_{2.5}$ and potential mechanisms. Ecotoxicol. Environ. Saf. 128, 67–74. https://doi.org/10.1016/j.ecoenv.2016.01.030

Gao, J., Woodward, A., Vardoulakis, S., Kovats, S., Wilkinson, P., Li, L., Xu, L., Li, J., Yang, J., Li, J., Cao, L., Liu, X., Wu, H., Liu, Q. (2017). Haze, public health and mitigation measures in China: A review of the current evidence for further policy response. Sci. Total Environ. 578, 148–157. https://doi.org/10.1016/j.scitotenv.2016.10.231

Gu, J., Zhang, Y. H., Yang, N., Wang, R. (2020). Diurnal variability of the planetary boundary layer height estimated from radiosonde data. Earth Planet. Phys. 4, 479–492. http://doi.org/10.26464/epp2020042

Guo, J., Miao, Y., Zhang, Y., Liu, H., Li, Z., Zhang, W., He, J., Lou, M., Yan, Y., Bian, L., Zhai, P. (2016). The climatology of planetary boundary layer height in China derived from radiosonde and reanalysis data. Atmos. Chem. Phys. 16, 13309–13319. https://doi.org/10.5194/acp-16-13309-2016

Guo, J., Su, T., Chen, D., Wang, J., Li, Z., Lv, Y., Guo, X., Liu, H., Cribb, M., Zhai, P. (2019). Declining Summertime Local-Scale Precipitation Frequency Over China and the United States, 1981–2012: The Disparate Roles of Aerosols. Geophys. Res. Lett. 46, 13281–13289. https://doi.org/10.1029/2019GL085442

Guo, J., Zhang, J., Yang, K., Liao, H., Zhang, S., Huang, K., Lv, Y., Shao, J., Yu, T., Tong, B., Li, J., Su, T., Yim, S.H.L., Stoffelen, A., Zhai, P., Xu, X. (2021). Investigation of near-global daytime boundary layer height using high-resolution radiosondes: first results and comparison with ERA5, MERRA-2, JRA-55, and NCEP-2 reanalyses. Atmos. Chem. Phys. 21, 17079–17097. https://doi.org/10.5194/acp-21-17079-2021

Holzworth, G.C. (1964). Estimates of mean maximum mixing depths in the contiguous United States. Mon. Weather Rev. 92, 235–242. https://doi.org/10.1175/1520-0493(1964)092<0235:EOMMMD>2.3.CO;2

Hu, X.M., Ma, Z., Lin, W., Zhang, H., Hu, J., Wang, Y., Xu, X., Fuentes, J.D., Xue, M. (2014). Impact of the Loess Plateau on the atmospheric boundary layer structure and air quality in the North China Plain: A case study. Sci. Total Environ. 499, 228–237. https://doi.org/10.1016/j.scitotenv.2014.08.053

Kampa, M., Castanas, E. (2008). Human health effects of air pollution. Environ. Pollut. 151, 362–367. https://doi.org/10.1016/j.envpol.2007.06.012

Kenessary, D., Kenessary, A., Adilgireiuly, Z., Akzholova, N., Erzhanova, A., Dosmukhametov, A., Syzdykov, D., Masoud, A.R., Saliev, T. (2019). Air Pollution in Kazakhstan and Its Health Risk Assessment. Ann. Global Health 85, 133. https://doi.org/10.5334/aogh.2535

Kerimray, A., Azbanbayev, E., Kenessov, B., Plotitsyn, P., Alimbayeva, D., Karaca, F. (2020a). Spatiotemporal variations and contributing factors of air pollutants in Almaty, Kazakhstan. Aerosol Air Qual. Res. 20, 1340–1352. https://doi.org/10.4209/aaqr.2019.09.0464

Kerimray, A., Assanov, D., Kenessov, B., Karaca, F. (2020b). Trends and health impacts of major urban air pollutants in Kazakhstan. J. Air Waste Manage. Assoc. 70, 1148–1164. https://doi.org/10.1080/10962247.2020.1813837

Koren, I., Dagan, G., Altaratz, O. (2014). From aerosol-limited to invigoration of warm convective clouds. Science 344, 1143–1146. https://doi.org/10.1126/science.1252595

Li, Z., Wang, Y., Guo, J., Zhao, C., Cribb, M.C., Dong, X., Fan, J., Gong, D., Huang, J., Jiang, M., Jiang, Y., Lee, S.S., Li, H., Li, J., Liu, J., Qian, Y., Rosenfeld, D., Shan, S., Sun, Y., Wang, H., *et al.* (2019a). East Asian study of tropospheric aerosols and their impact on regional clouds, precipitation, and climate (EAST-AIR CPC). J. Geophys. Res. 124, 13026–13054. https://doi.org/10.1029/2019JD030758

Li, R., Wang, Z., Cui, L., Fu, H., Zhang, L., Kong, L., Chen, W., Chen, J. (2019b). Air pollution characteristics in China during 2015-2016: Spatiotemporal variations and key meteorological factors. Sci. Total Environ. 648, 902–915. https://doi.org/10.1016/j.scitotenv.2018.08.181

Met One Instruments (2021). Continuous Particulate Monitor BAM 1020. https://metone.com/products/bam-1020/

Miao, Y., Liu, S., Guo, J., Huang, S., Yan, Y., Lou, M. (2018). Unraveling the relationships between boundary layer height and $PM_{2.5}$ pollution in China based on four-year radiosonde measurements. Environ. Pollut. 243, 1186–1195. https://doi.org/10.1016/j.envpol.2018.09.070

Nielsen-Gammon, J.W., Powell, C.L., Mahoney, M.J., Angevine, W.M., Senff, C., White, A., Berkowitz, C., Doran, C., Knupp, K. (2008). Multisensor estimation of mixing heights over a coastal city. J. Appl. Meteorol. Climatol. 47, 27–43. https://doi.org/10.1175/2007JAMC1503.1

Ormanova, G., Karaca, F., Zhumabayeva, E. (2020). Valuation of Global Data Assimilation System (GDAS) atmospheric stability forecast data usage on short term $PM_{2.5}$ predictions. Title of the conference: Air & Waste Management Association (AWMA) 113th Annual Conference & Exhibition (ACE), https://www.eventscribe.com/2020/ACEVIRTUAL/fsPopup.asp?Mode=presInfo&PresentationID=739116

Permadi, D.A., Oanh, N.T.K., Vautard, R. (2018a). Assessment of emission scenarios for 2030 and impacts of black carbon emission reduction measures on air quality and radiative forcing in Southeast Asia. Atmos. Chem. Phys. 18, 3321–3334. https://doi.org/10.5194/acp-18-3321-2018

Permadi, D.A., Oanh, N.T.K., Vautard, R. (2018b). Integrated emission inventory and modeling to assess distribution of particulate matter mass and black carbon composition in Southeast Asia, Atmos. Chem. Phys. 18, 2725–2747. https://doi.org/10.5194/acp18-2725-2018

Pogoda i Climate (2021). Klimat Almaty. http://www.pogodaiklimat.ru/climate/36870.htm

Russell, A., Ghalaieny, M., Gazdiyeva, B., Zhumabayeva, S., Kurmanbayeva, A., Akhmetov, K.K., Mukanov, Y., McCann, M., Ali, M., Tucker, A., Vitolo, C., Althonayan, A. (2018). A spatial survey of environmental indicators for Kazakhstan: An Examination of current conditions and future needs. Int. J. Environ. Res. 12, 735–748. https://doi.org/10.1007/s41742-018-0134-7

Seibert, P., Beyrich, F., Gryning, S.E., Joffre, S., Rasmussen, A., Tercier, P. (2000). Review and intercomparison of operational methods for the determination of the mixing height. Atmos. Environ. 34, 1001–1027. https://doi.org/10.1016/S1352-2310(99)00349-0

Seidel, D.J., Zhang, Y., Beljaars, A., Golaz, J.C., Jacobson, A.R., Medeiros, B. (2012). Climatology of the planetary boundary layer over the continental United States and Europe. J. Geophys. Res. 117, D17106. https://doi.org/10.1029/2012JD018143

Statista (2021). Average annual $PM_{2.5}$ air pollution levels in Beijing, China between 2010 and 2020. https://www.statista.com/statistics/690823/china-annual-pm25-particle-levels-beijing/

Su, T., Li, Z., Zheng, Y., Luan, Q., Guo, J. (2020). Abnormally shallow boundary layer associated with severe air pollution during the COVID-19 lockdown in China. Geophys. Res. Lett. 47, e2020GL090041. https://doi.org/10.1029/2020GL090041

University of Wyoming (2020). Aerological stations. http://weather.uwyo.edu/upperair/sounding.html

Vinnikov, D., Tulekov, Z., Raushanova, A. (2020). Occupational exposure to particulate matter from air pollution in the outdoor workplaces in Almaty during the cold season. PLoS One 15, e0227447. https://doi.org/10.1371/journal.pone.0227447

Wang, H., Xu, J., Zhang, M., Yang, Y., Shen, X., Wang, Y., Chen, D., Guo, J. (2014). A study of the meteorological causes of a prolonged and severe haze episode in January 2013 over central-eastern China. Atmos. Environ. 98, 146–157. https://dio.org/10.1016/j.atmosenv.2014.08.053

Wang, M., Kai, K., Jin, Y., Sugimoto, N., Dashdondog, B. (2017). Air particulate pollution in Ulaanbaatar, Mongolia: Variation in atmospheric conditions from autumn to winter. SOLA 13, 90–95. https://doi.org/10.2151/sola.2017-017

Weather Schedule (2021). Weather in 243 countries. http://rp5.kz

World Health Organization (WHO) (2021). Ambient (outdoor) air pollution. https://www.who.int/news-room/fact-sheets/detail/ambient-(outdoor)-air-quality-and-health

WHO Regional Office for Europe, OECD (2015). Economic cost of the health impact of air pollution in Europe: Clean air, health and wealth. WHO Regional Office for Europe, Copenhagen.

Yin, P., Guo, J., Wang, L., Fan, W., Lu, F., Guo, M., Moreno, S.B.R., Wang, Y., Wang, H., Zhou, M., Dong, Z. (2020). Higher risk of cardiovascular disease associated with smaller size-fractioned particulate matter. Environ. Sci. Technol. Lett. 7, 95–101. https://doi.org/10.1021/acs.estlett.9b00735